Select G-Protein-Coupled Receptors Modulate Agonist-Induced Signaling via a ROCK, LIMK, and β-Arrestin 1 Pathway

Nitish Mittal,[1,7] Kristofer Roberts,[1,7] Katsuri Pal,[2] Laurent A. Bentolila,[3,6] Elissa Fultz,[1] Ani Minasyan,[1] Catherine Cahill,[4] Amynah Pradhan,[1] David Conner,[5] Kathryn DeFea,[2] Christopher Evans,[1] and Wendy Walwyn[1,*]

[1]Department of Psychiatry and Biobehavioral Sciences, Stefan Hatos Center for Neuropharmacology, Semel Institute, University of California, Los Angeles, Los Angeles, CA 90095, USA
[2]Division of Biomedical Sciences, Cell, Molecular, and Developmental Biology Program, University of California, Riverside, Riverside, CA 92521, USA
[3]Department of Chemistry and Biochemistry, University of California, Los Angeles, Los Angeles, CA 90095, USA
[4]Department of Anesthesiology and Perioperative Care, University of California, Irvine, Irvine, CA 92697, USA
[5]Department of Genetics, Harvard Medical School, Boston, MA 02115, USA
[6]California NanoSystems Institute, University of California, Los Angeles, Los Angeles, CA 90095, USA
[7]These authors contributed equally to this work
*Correspondence: wwalwyn@ucla.edu
http://dx.doi.org/10.1016/j.celrep.2013.10.015

SUMMARY

G-protein-coupled receptors (GPCRs) are typically present in a basal, inactive state but, when bound to an agonist, activate downstream signaling cascades. In studying arrestin regulation of opioid receptors in dorsal root ganglia (DRG) neurons, we find that agonists of delta opioid receptors (δORs) activate cofilin through Rho-associated coiled-coil-containing protein kinase (ROCK), LIM domain kinase (LIMK), and β-arrestin 1 (β-arr1) to regulate actin polymerization. This controls receptor function, as assessed by agonist-induced inhibition of voltage-dependent Ca^{2+} channels in DRGs. Agonists of opioid-receptor-like receptors (ORL1) similarly influence the function of this receptor through ROCK, LIMK, and β-arr1. Functional evidence of this cascade was demonstrated in vivo, where the behavioral effects of δOR or ORL1 agonists were enhanced in the absence of β-arr1 or prevented by inhibiting ROCK. This pathway allows δOR and ORL1 agonists to rapidly regulate receptor function.

INTRODUCTION

The neuronal cytoskeleton provides both the 3D structural stability critical for cellular function and the infrastructure that allows the cell to respond to external stimuli. Dynamic remodeling of the cytoskeleton, particularly of the actin filaments, provides the network along which intracellular proteins may be trafficked as needed. This mechanism allows proteins to be shuttled to and from the synapse and allows the Golgi apparatus to sort and traffic newly synthesized proteins to the cell membrane (Lowe, 2011; Salvarezza et al., 2009). Proteins bound for the cell membrane from the Golgi may be either constitutively exported through a specific pathway with specialized secretory vesicles that are formed and move continuously along the microtubules or secreted on demand. A dynamic actin cytoskeleton plays an important role in this process; both the actin-severing protein cofilin, and the upstream kinase LIMK, have been shown to inhibit or facilitate the release of specific proteins from the Golgi to the cell membrane (Egea et al., 2006; Heimann et al., 1999; Salvarezza et al., 2009).

Similar to many other membrane proteins, newly synthesized G-protein-coupled receptors (GPCRs) are sorted, processed, degraded, or trafficked from the endoplasmic reticulum to the Golgi. Thereafter, GPCR transfer through the Golgi stack is complex and may involve several escort or chaperone proteins to release the receptor to the cell membrane. For the most part, the rate of GPCR release to the cell membrane is determined by the quality-control mechanisms within the endoplasmic reticulum, and once within the Golgi, GPCRs are presumed to be constitutively released to the cell membrane. By regulating the number of GPCRs released to the cell membrane, this biosynthetic pathway may influence receptor availability and signaling (Achour et al., 2008; Dong et al., 2007).

β-arrestin 1 or 2 recruitment to the protease-activated receptor 2 (PAR₂) regulates chemotaxis by binding with and activating cofilin and associated regulatory proteins. This alters actin turnover within the leading and trailing edges of the cell in order to facilitate cell migration (DeFea, 2007; Xiao et al., 2010; Zoudilova et al., 2007, 2010). In examining β-arrestin 1 (β-arr1) regulation of GPCR function in dorsal root ganglia (DRG) neurons, we have found that this arrestin isoform influences the stability of the actin cytoskeleton to rapidly control the magnitude of GPCR signaling.
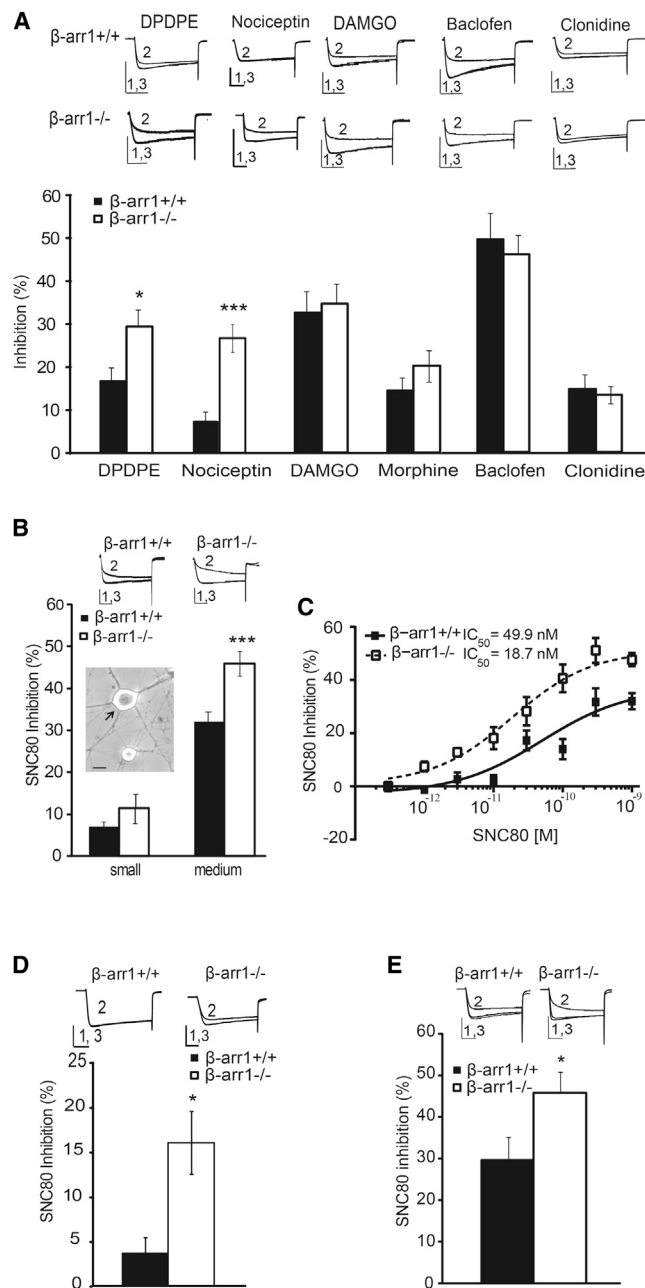
Figure 1. δOR and ORL1 Function Is Enhanced in Dorsal Root Ganglia Neurons Lacking β-arr1

(A) The whole-cell patch-clamp technique was used to examine VDCC inhibition by $G_{o/i}$ coupled receptors. DPDPE, a peptidergic δOR agonist, and nociceptin, an ORL1 agonist, demonstrated enhanced VDCC coupling in β-arr1$^{-/-}$ versus β-arr1$^{+/+}$ DRG neurons, whereas VDCC inhibition by agonists of the mu receptor, DAMGO and morphine (1 μM ea), the GABA$_B$ receptor, baclofen (50 μM), and the α_{2A} receptor, clonidine (10 μM), was not different across genotypes.

(B) Further analysis of δOR-VDCC inhibition showed enhanced δOR inhibition of VDCCs by the nonpeptidergic δOR agonist, SNC80, in medium (shown by the arrow), but not small, early postnatal medium-sized β-arr1$^{-/-}$ versus β-arr1$^{+/+}$ DRG neurons in the SvEv129SJ background. Scale bar = 10 μm.

(C) The concentration response curve demonstrated enhanced efficacy and potency of SNC80 in β-arr1$^{-/-}$ versus β-arr1$^{+/+}$ neurons (p < 0.001).

RESULTS

The primary afferent neurons of the DRGs, the first-order neurons of the analgesic pathway, relay nociceptive information from the peripheral to the central nervous system. In addition to a number of $G_{i/o}$-coupled GPCRs, these neurons also express the nonvisual arrestins (Komori et al., 1999). Of the two isoforms, β-arrestin 2 is known to regulate the function of some $G_{i/o}$-coupled GPCRs in DRG neurons (Tan et al., 2009; Walwyn et al., 2007). However, whether β-arr1 regulates the function of these GPCRs has not been established.

β-arr1 Modulates VDCC Inhibition by Some GPCRs

As agonists of $G_{i/o}$-coupled GPCRs can inhibit voltage-dependent Ca^{2+} channels (VDCC), the whole-cell patch-clamp technique was used to assess β-arr1 regulation of $G_{i/o}$-coupled GPCRs in DRG neurons. Of the five GPCRs examined, we found that VDCC inhibition by the δOR agonist, DPDPE (p < 0.05 versus β-arr1$^{+/+}$), and the ORL1 agonist, nociceptin (p < 0.001 versus β-arr1$^{+/+}$), was enhanced in cells lacking β-arr1. On the other hand, VDCC inhibition by agonists of the mu opioid and GABA$_B$ and α_{2A} adrenergic receptors was not altered (Figure 1A). Further analysis of the δOR-VDCC profile showed that, in addition to the peptidergic agonist, DPDPE, the nonpeptidergic and arguably more selective δOR agonist, SNC80 (1 μM), also resulted in greater VDCC inhibition in medium-sized, but not small, DRG neurons lacking β-arr1 (p < 0.001 versus β-arr1$^{+/+}$; Figure 1B). The concentration-response curve of SNC80 in medium-sized neurons demonstrated enhanced efficacy and potency of this δOR agonist in β-arr1$^{-/-}$ neurons (Emax; β-arr1$^{+/+}$; 32.1 ± 3.1, β-arr1$^{-/-}$; 47.7% ± 2.5% inhibition, p < 0.001; Figure 1C). This enhanced inhibition was receptor specific; it was reversed by the delta antagonist naltrindole (NTI; SNC80 and NTI applied at 1 μM; β-arr1$^{+/+}$; 0.1% ± 0.6%, β-arr1$^{-/-}$; 1.1% ± 1.8% inhibition). It was also reversed by the ORL1 antagonist, JTC801 (JTC801 and nociceptin at 1 μM: β-arr1$^{+/+}$; 1.6% ± 7.1%, β-arr1$^{-/-}$; 6.3% ± 5.1%). Medium-sized neurons from mice of different ages or backgrounds showed the same profile of enhanced inhibition in β-arr1$^{-/-}$ neurons (p < 0.05 versus β-arr1$^{+/+}$; Figures 1D and 1E), which could not be explained by basal changes in Ca^{2+} channel density, the relative proportion of N-, P/Q-, and L-type Ca^{2+} channels present, or constitutive δOR-VDCC coupling (Figure S1).

β-arr1 Regulation of δOR Desensitization

As δORs recruit β-arr1 or β-arr2 and show less desensitization in cells lacking β-arr1 (Qiu et al., 2007), the enhanced efficacy of

(D) Similar to neurons from mice backcrossed into the SvEv129SJ background, medium-sized DRG neurons from early postnatal β-arr1$^{-/-}$ in the C57Bl/6 background showed enhanced SNC80-VDCC inhibition.

(E) Similar to early postnatal DRG neurons, medium-sized DRG neurons from adult mice showed increased SNC80-VDCC inhibition in β-arr1$^{-/-}$ versus β-arr1$^{+/+}$ neurons.

All data are shown as mean ± SEM. *p < 0.05 versus β-arr1$^{+/+}$; **p < 0.001 versus β-arr1$^{+/+}$; ***p < 0.001 versus β-arr1$^{+/+}$; n = 6–27 per data point. All exemplar currents depict the current before (1), during (2), and after (3) agonist application, and the scale bars show time (20 ms) on the x axis and current on the y axis (5 or 10 nA) for early postnatal or adult DRG neurons, respectively.
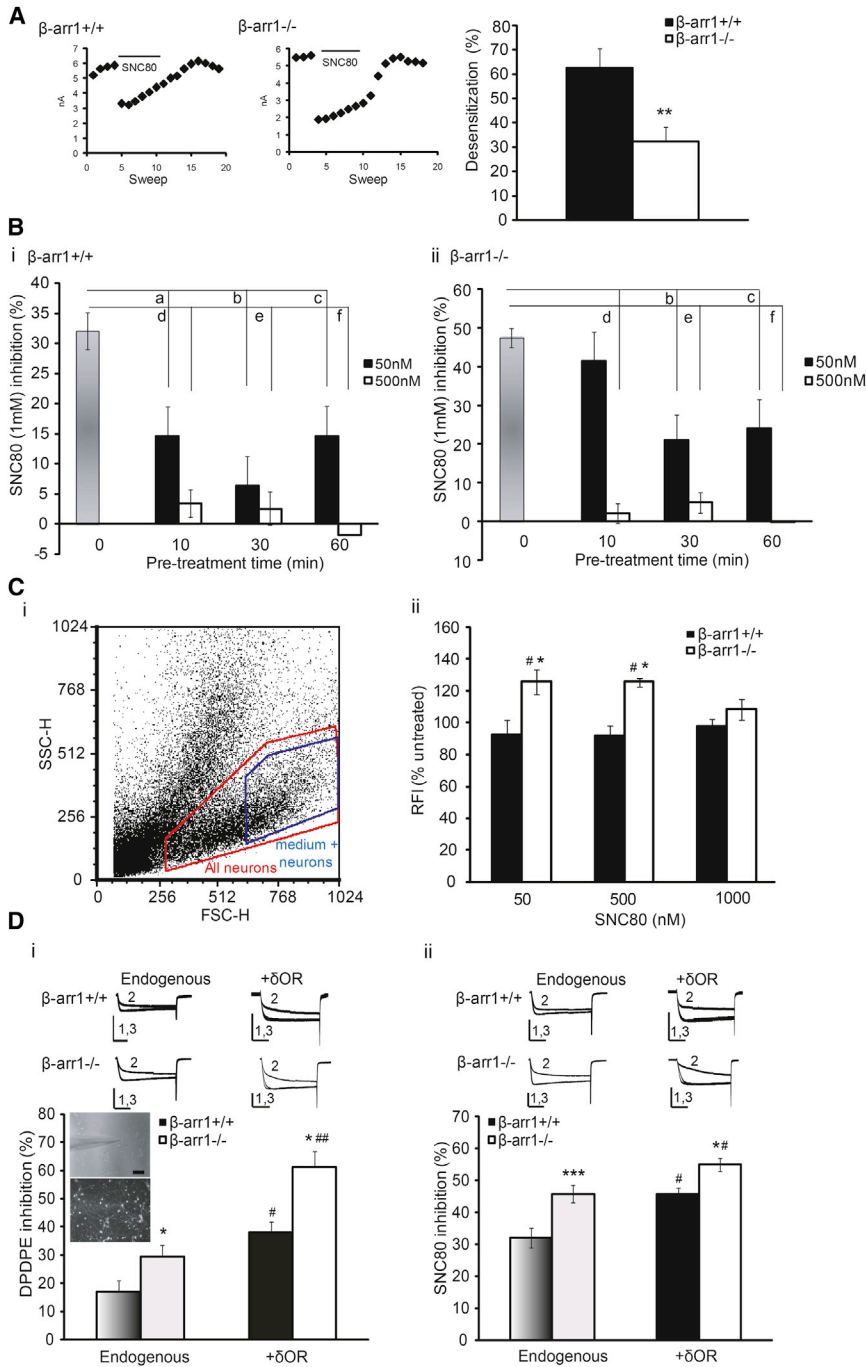
Figure 2. β-arr1 Regulates δOR Desensitization and Internalization, but This Does Not Explain the Enhanced δOR-VDCC Coupling in β-arr1−/− Neurons

(A) Rapid desensitization. Once complete inhibition of VDCCs was obtained by SNC80, further perfusion with SNC80 desensitized this inhibition. This is shown by the decline in the peak current amplitude over 120 s in the left panels. Although both β-arr1+/+ and β-arr1−/− neurons desensitized, β-arr1−/− neurons showed less desensitization. **p < 0.01; n = 5–10.

(B) Acute desensitization. Whereas preincubation of DRGs with 50 and 500 nM SNC80 for 10 min desensitized δOR-VDCC inhibition at all time points in +/+ neurons, −/− neurons did not desensitize after 10 min of 50 nM SNC80 but desensitized thereafter and showed equivalent desensitization at all time points when preincubated with 500 nM SNC80. β-arr1+/+: a, b, and c: p < 0.05 versus untreated; d and e: p < 0.0001 versus untreated; f: p < 0.001 versus untreated. β-arr1−/−: b: p < 0.001 versus untreated; c: p < 0.001 versus untreated; d, e, f: p < 0.0001 versus untreated; n = 6–7 per data point. Columns in shades of gray, Bi; +/+ or Bii; −/−, indicate data shown in Figure 1.

(C) Internalization assessed by flow cytometry in β-arr1−/− and β-arr1+/+ DRG neurons using an N-terminal antibody and allophycocyanin (APC)-conjugated secondary antibody. (i) The δOR-labeled nonfixed samples were initially sorted by size (FSC-H) and granularity (SSC-H) to select the medium-large DRG neurons (>25 μM in diameter; Walwyn et al., 2004). APC-labeled δORs were then selected after removing nonspecific background labeling and all samples of each experiment analyzed by these parameters. (ii) Although basal cell surface δOR levels were unaffected by the β-arr1−/− deletion, 50 and 500 nM SNC80, but not 1,000 nM SNC80, increased cell surface δOR levels in βarr1−/− DRGs. #p < 0.05 versus untreated β-arr1−/−; *p < 0.05 versus β-arr1+/+, same time point; n = 4–8 per data point.

(D) A slower rate of internalization could enhance δOR-VDCC inhibition by increasing the number of δORs on the plasma membrane. This was assessed by overexpressing cerulean (CFP)-labeled δORs (Walwyn et al., 2009). This increased δOR-VDCC inhibition equally in both β-arr1+/+ and β-arr1−/− neurons tested with either DPDPE or SNC80 (1 μM ea). *p < 0.05, **p < 0.01, and ***p < 0.001 versus β-arr1+/+; #p < 0.05 and ## p < 0.01 versus endogenous δORs; n = 6–18 per data point. All exemplar currents depict the current before, during, and after agonist application (1, 2, and 3) and the scale bars show time (20 ms) and current (5 nA) on the x and y axes, respectively. Columns in dark (β-arr1+/+) or light (β-arr1−/−) shades of gray indicate data shown in Figure 1. All data are shown as mean ± SEM.

δOR agonists in β-arr1−/− neurons could be a result of attenuated desensitization. This was assessed in vitro by rapid desensitization, in which an agonist is continually perfused while δOR-VDCC inhibition is monitored, and by acute desensitization, in which the cells are preincubated with SNC80, washed, and δOR-VDCC inhibition assessed. Both measures showed a genotype effect (Figures 2A and 2B). First, rapid desensitization

occurred in both β-arr1−/− and β-arr1+/+ neurons, but this was less in β-arr1−/− neurons (p < 0.01 versus β-arr1+/+; Figure 2A). Second, acute desensitization, involving preincubation with 50 or 500 nM of SNC80 for 10, 30, or 60 min, followed by a 1 μM SNC80 test dose, showed delayed desensitization after 10 min of 50 nM SNC80 in βarr1−/− neurons but equivalent desensitization thereafter and no difference in the amount or rate of
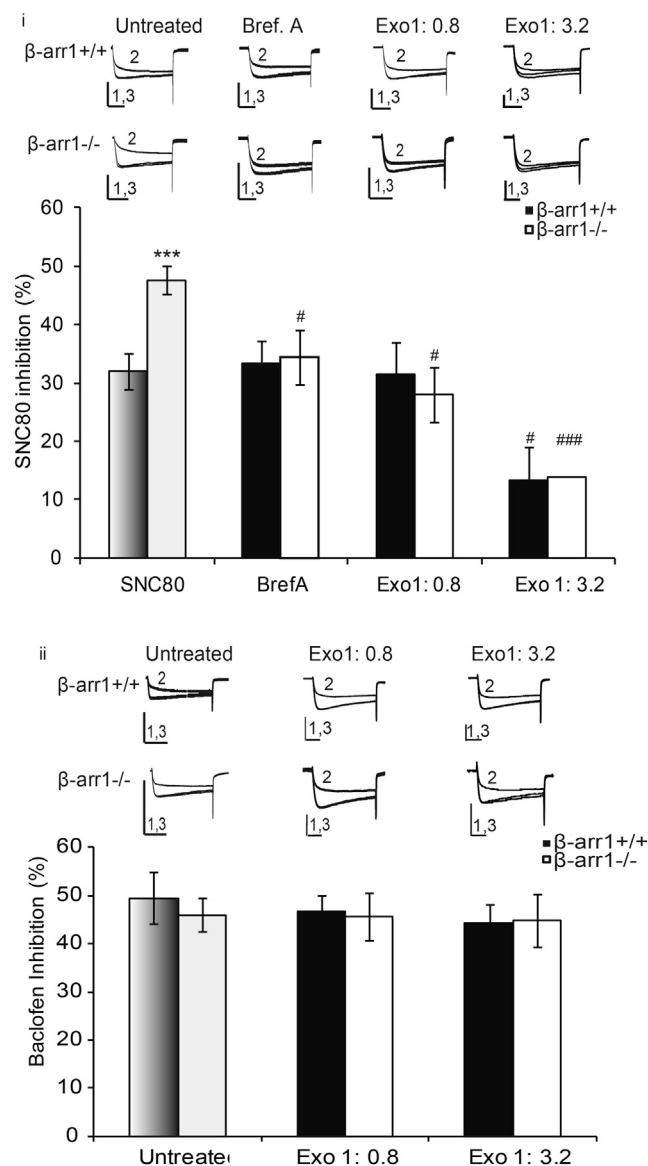
Figure 3. β-arr1 Control of Protein Export Explains Enhanced δOR-VDCC Inhibition

The increase in cell surface receptor number after 50 and 500 nM SNC80 (Figure 2C) could reflect β-arr1 control of δOR release to the plasma membrane. This was assessed by inhibiting protein export. (i) DRGs were pretreated with brefeldin A (Bref. A; 1 μg/ml 30 min pretreatment) to inhibit protein release from the endoplasmic reticulum and Exo1, a more specific inhibitor of protein release from the Golgi (0.8 and 3.2 μg/ml, included in the intracellular recording solution). Both brefeldin A and Exo1 (0.8 μg/ml) reduced the enhanced SNC80 inhibition of VDCCs in β-arr1$^{-/-}$ to β-arr1$^{+/+}$ levels, but the higher dose of Exo1 (3.2 μg/ml) reduced SNC80-inhibition in both −/− and +/+ neurons. (ii) Exo1 did not affect GABA$_B$-VDCC inhibition, assessed by baclofen (50 μM).

All data are shown as mean ± SEM. #p < 0.05 versus untreated β-arr1$^{+/+}$ or β-arr1$^{-/-}$. ***p < 0.001 versus β-arr1$^{+/+}$; n = 6–12 per data point All exemplar currents depict the current before, during, and after agonist application (1, 2, and 3) and the scale bars show time (20 ms) and current (5 nA) on the x and y axes, respectively. Columns in dark (β-arr1$^{+/+}$) or light (β-arr1$^{-/-}$) shades of gray indicate data shown in Figure 1.

desensitization induced by 500 nM SNC80 (Figure 2B). In summary, we found that δOR desensitization was delayed in β-arr1$^{-/-}$ neurons. However, when compared with δOR-VDCC inhibition, which reached a maximum within 20–40 s of agonist exposure, the attenuated desensitization, seen by 120 s of continual agonist perfusion, cannot explain the enhanced δOR-VDCC inhibition seen in β-arr1$^{-/-}$ neurons.

β-arr1 Regulation of δOR Internalization

As the arrestins are known to initiate internalization, deleting β-arr1 could delay δOR internalization to increase cell surface receptor number and enhance δOR function. Internalization was examined by flow cytometry using an allophycocyanin-labeled antibody to the N terminus of the δOR, the specificity of which was confirmed in cells lacking δORs (Figure S2). The nonfluorescent parameters of size and granularity were then used to gate on medium- to large-sized neurons (Figure 2Ci; Walwyn et al., 2004). These cells showed no effect of genotype on basal cell surface receptor levels (β-arr1$^{-/-}$: 89.9 ± 4.0 of β-arr1$^{+/+}$ levels). However, after 10 min of 50 and 500 nM SNC80, but not 1 μM SNC80, cell surface receptor levels were increased in β-arr1$^{-/-}$ (p < 0.05 versus untreated β-arr1$^{-/-}$), but not β-arr1$^{+/+}$, neurons (p < 0.05 versus β-arr1$^{+/+}$; Figure 2Cii). After 1 hr of SNC80 (1 μM), virally expressed cerulean-labeled δORs expressed in β-arr1$^{+/+}$ and β-arr1$^{-/-}$ neurons demonstrated significant internalization (Figure S3). As δORs are dynamically trafficked to and from the cell membrane, the initial increase in δORs on the cell membrane could reflect delayed internalization and/or enhanced externalization in β-arr1$^{-/-}$ neurons (Cahill et al., 2007; Walwyn et al., 2009).

Accumulation of δORs on the Cell Membrane Does Not Account for the Enhanced δOR Function in β-arr1$^{-/-}$ Neurons

Attenuated internalization or enhanced externalization would lead to an accumulation of receptors on the cell membrane, so explaining the increase in δOR-VDCC coupling in β-arr1$^{-/-}$ neurons. Lentiviral expression of cerulean-tagged (CFP) δORs was therefore used to overexpress δORs in β-arr1$^{-/-}$ and β-arr1$^{+/+}$ neurons. This did increase δOR-VDCC inhibition, assessed by either 1 μM DPDPE or 1 μM SNC80 (p < 0.05 versus endogenous levels; Figure 2D). However, the increase occurred equally in β-arr1$^{+/+}$ and β-arr1$^{-/-}$ neurons, suggesting that δOR-VDCC inhibition is sensitive to altered receptor number but that the regulatory role of β-arr1 remains even when these receptors are overexpressed (p < 0.05 versus β-arr1$^{+/+}$).

β-arr1 Control of Protein Export Explains the Enhanced δOR-VDCC Inhibition

Because flow cytometric analysis showed a greater number of δORs on the cell membrane, it is possible that β-arr1 controls δOR release to the cell membrane in an agonist-dependent manner. This was tested by preincubating cells with brefeldin A, an inhibitor of protein export. This reduced δOR-VDCC inhibition in β-arr1$^{-/-}$ neurons to β-arr1$^{+/+}$ levels with no effect in +/+ neurons at this concentration (p < 0.05 versus untreated β-arr1$^{-/-}$; Figure 3i). A more specific inhibitor of protein export

from the Golgi, ExoI (0.8 μg/ml), reduced δOR-VDCC inhibition in β-arr1$^{-/-}$ neurons and, when used at a higher concentration (3.2 μg/ml), reduced δOR-VDCC inhibition in both β-arr1$^{+/+}$ and β-arr1$^{-/-}$ neurons (p < 0.05 versus untreated; Figure 3ii). To probe for nonspecific effects, GABA$_B$-VDCC was examined in the presence of ExoI, but no effect was found (Figure 3iii). As δOR-VDCC inhibition is closely correlated with cell surface receptor levels (Walwyn et al., 2005), these data could be interpreted as an Exo1-mediated inhibition of δORs released to the cell membrane in an agonist-dependent manner.

δOR Activation of Cofilin Is β-arr1 Dependent

Both LIMK and cofilin are required for the export of specific proteins from the Golgi to the cell membrane (Salvarezza et al., 2009; von Blume et al., 2009). δORs could activate cofilin to regulate receptor export via this pathway and to affect receptor function. δOR activation of the phosphorylated, inactivated form of cofilin was assessed in mouse embryonic fibroblasts (MEFs). MEFs were chosen for this assay because they express or lack the necessary proteins of this pathway (β-arr1, ROCK, LIMK, and cofilin) and have been used to study arrestin-GPCR signaling (Zoudilova et al., 2010). This pathway is also conserved in DRGs (Ahmed et al., 2011). In wild-type MEFs, we found that SNC80 (1 μM) reduced the amount of phosphorylated cofilin in β-arr1$^{-/-}$ (2–30 min; p < 0.01 or 0.01 versus untreated β-arr1$^{+/+}$), but not in β-arr1$^{+/+}$, MEFs. Together, these data show that SNC80 activates cofilin in a β-arr1-dependent manner (Figure 4A).

ROCK, LIMK, and β-arr1 Regulation of δOR-VDCC Coupling

Given that β-arr1 is known to bind with and regulate LIMK (Zoudilova et al., 2007) and LIMK has been shown to control the export of specific proteins from the Golgi (Salvarezza et al., 2009), it is possible that δOR export and therefore function may be regulated by β-arr1. We examined this possibility by inhibiting ROCK, the kinase responsible for phosphorylating and activating LIMK, in neurons containing or lacking β-arr1. The ROCK inhibitor Y27632 decreased δOR-VDCC inhibition in both β-arr1$^{-/-}$ and β-arr1$^{+/+}$ neurons (p < 0.01 versus untreated β-arr1$^{+/+}$; p < 0.001 vs untreated β-arr1$^{-/-}$; Figure 4B) but had no effect on GABA$_B$-VDCC coupling (untreated: β-arr1$^{+/+}$; 49.8% ± 5.3%, β-arr1$^{-/-}$: 46.6% ± 3.4%, Y27632 (400 ng/ml); β-arr1$^{+/+}$; 49.5% ± 2.2%, β-arr1$^{-/-}$: 51.1% ± 2.5%). We then used an approach designed to enhance LIMK activity by including excess LIMK (1 and 2 μg/ml) within the intracellular recording solution. The 2 μg/ml dose increased δOR-VDCC coupling in both β-arr1$^{+/+}$ and β-arr1$^{-/-}$ neurons (p < 0.05 versus untreated β-arr1$^{+/+}$ or β-arr1$^{-/-}$; Figure 4B), demonstrating that LIMK influence δOR-VDCC inhibition. Because LIMK phosphorylation of cofilin can be inhibited by the serine 3 LIMK peptide (Aizawa et al., 2001), we included this peptide in the intracellular recording solution (S3; 1.6 and 6.4 μg/ml). This reduced δOR-VDCC inhibition in β-arr1$^{-/-}$ neurons (p < 0.001 versus untreated β-arr1$^{-/-}$), but not in β-arr1$^{+/+}$ neurons (Figure 4B). Together, these data suggest that δOR-VDCC inhibition may be regulated by ROCK, LIMK, and β-arr1.

Actin Polymerization Influences δOR-VDCC Inhibition

LIMK has been shown to phosphorylate and inhibit cofilin to stabilize the actin cytoskeleton in dendritic spines (Shi et al., 2009). It is possible that LIMK, β-arr1, and cofilin could similarly regulate the stability of the actin "tracks" required for the export of δORs to the cell membrane. The ability of actin polymerization to affect δOR-VDCC inhibition was therefore examined by manipulating actin polymerization minutes before assessing δOR-VDCC inhibition. First, we stabilized the actin cytoskeleton by including jasplakinolide and thymosin β4 within the intracellular recording solution (Bubb et al., 1994; Huff et al., 2001). This increased δOR-VDCC inhibition in β-arr1$^{+/+}$ neurons to β-arr1 levels but had no effect in neurons (p < 0.05 versus untreated β-arr1$^{+/+}$; Figure 4C). Preventing polymerization by including latrunculin B (LatB, 200 ng/ml; Morton et al., 2000) within the intracellular recording solution reduced the enhanced δOR-VDCC inhibition in β-arr1$^{-/-}$ neurons to β-arr1$^{+/+}$ levels without affecting GABA$_B$-VDCC inhibition (p < 0.05 versus untreated β-arr1$^{-/-}$; Figure 4C). Together, these data demonstrate that manipulations designed to influence actin polymerization can regulate SNC80-VDCC inhibition.

ORL1-VDCC Inhibition Is Similarly Controlled by β-arr1, ROCK, LIMK, and Actin Polymerization

The previous experiments used δORs as a model GPCR to examine each component of this regulatory pathway. Because ORL1-VDCC inhibition was upregulated in β-arr1$^{-/-}$ neurons, we next examined whether, similar to δORs, ORL1-VDCC may be controlled by this ROCK-LIMK pathway in a β-arr1-dependent manner. We assessed the effect of inhibitors of this pathway (Y27632 [400 ng/ml], S3 [6.4 μg/ml], or LatB [200 nM]) on ORL1-VDCC coupling in β-arr1$^{-/-}$ and β-arr1$^{+/+}$ DRG neurons. These three compounds reversed the enhanced ORL1-VDCC inhibition in −/− neurons (p < 0.001 versus untreated β-arr1$^{-/-}$) but had no effect in +/+ neurons (Figure 4D). These data suggest that ORL1-VDCC coupling may be controlled by ROCK, LIMK, and actin polymerization in the absence of β-arr1$^{-/-}$.

Basal F-actin Incorporation Appears Unchanged

Because deleting β-arr1 could alter basal LIMK and cofilin activity, this could affect actin turnover throughout the cell. This was assessed by the incorporation of Atto-647N phalloidin (30 nM, 10 min) in living DRG neurons that were then fixed and analyzed by stimulated emission depletion (STED) microscopy. No effect of genotype on phalloidin incorporation was observed in either the neuronal cell bodies or processes of β-arr1$^{-/-}$ versus β-arr1$^{+/+}$ neurons, suggesting that basal actin polymerization was not altered in β-arr1 DRGs (Figure S4).

Behavioral Assays Provide Functional Evidence for the Role of ROCK and β-arr1 in Regulating δOR and ORL1 Function
δOR

Two well-known behavioral assays of δOR function, locomotion and analgesia, were used to assess the function of this pathway. In the open-field test of locomotion, SNC80 (3 mg/kg administered subcutaneously [s.c.]) increased the locomotor activity of
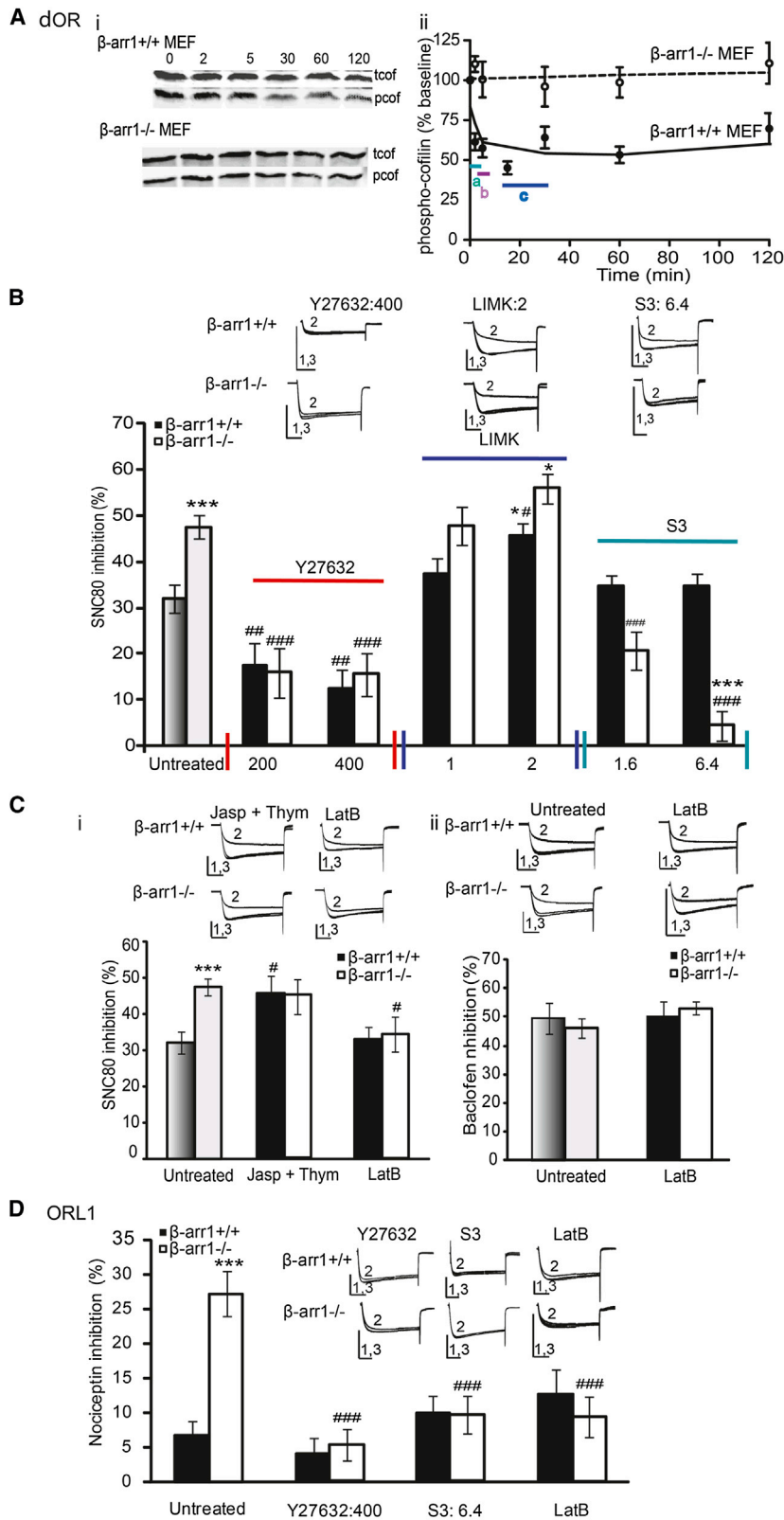
Figure 4. δOR and ORL1 Inhibition of VDCCs Is Regulated by LIMK, ROCK, and Actin Polymerization

(A) The δOR agonist, SNC80, activates cofilin. Wild-type MEFs (WT MEFs) or β-arr1$^{-/-}$ MEFs were treated with SNC80 for 0–120 min and lysates analyzed by western blot. (i) Representative western blots of phosphorylated cofilin (pcof) and total cofilin (tcof) in WT MEFs (upper two panels) and β-arr1$^{-/-}$ MEFs (lower two panels) after SNC80 treatment. (ii) SNC80 (1 μM) decreased phosphocofilin after 2, 5, 15, and 30 min in WT MEFs (closed circles), whereas β-arr1$^{-/-}$ MEFs (open circles) showed no change. Values on the y axis represent phosphocofilin normalized to basal levels at each time point shown on the x axis. A: $p < 0.001$; b: $p < 0.01$; c: $p < 0.01$ versus untreated WT MEFs.

(B) The ROCK inhibitor, Y27632 (200 and 400 ng/ml), reduced δOR-VDCC coupling in β-arr1$^{-/-}$ and β-arr1$^{+/+}$ neurons. Although excess LIMK (2 μg/ml) increased SNC80-VDCC inhibition in both β-arr1$^{+/+}$ and β-arr1$^{-/-}$ neurons, SNC80-VDCC inhibition remained higher in β-arr1$^{-/-}$ neurons. LIMK phosphorylation of cofilin can be prevented by the serine 3 peptide. This decreased SNC80-VDCC inhibition in β-arr1$^{-/-}$ neurons, but not β-arr1$^{+/+}$ neurons (S3: 1.6 and 6.4 ng/ml).

(C) (i) Jasplakinolde and thymosin B4 (200 ng/ml), enhancers of actin polymerization, increased SNC80-VDCC inhibition in β-arr1$^{+/+}$ to β-arr1$^{-/-}$ levels, whereas latrunculin B (LatB; 200 ng/ml), an inhibitor of actin polymerization, reversed the increased δOR-VDCC inhibition in β-arr1$^{-/-}$ to β-arr1$^{+/+}$ levels. (ii) LatB did not alter GABA$_B$-VDCC inhibition assessed by baclofen (50 μM).

(D) The increase in ORL1-VDCC inhibition in β-arr1$^{-/-}$ DRG neurons was reversed by the ROCK inhibitor, Y27632 (400 ng/ml), the LIMK inhibitory peptide, S3 (6.4 ng/ml), and latrunculin B (200 ng/ml). No effect of these manipulations was seen in +/+ neurons.

All data are shown as mean ± SEM. *$p < 0.05$ and ***$p < 0.001$ versus β-arr1$^{+/+}$; ##$p < 0.01$ or ###$p < 0.001$ versus untreated, matched genotype; n = 6–12 per data point. All exemplar currents depict the current before, during, and after agonist application (1, 2, and 3) and the scale bars show time (20 ms) and current (5 nA) on the x and y axes, respectively. Columns in dark (β-arr1$^{+/+}$) or light (β-arr1$^{-/-}$) shades of gray indicate data shown in Figure 1.
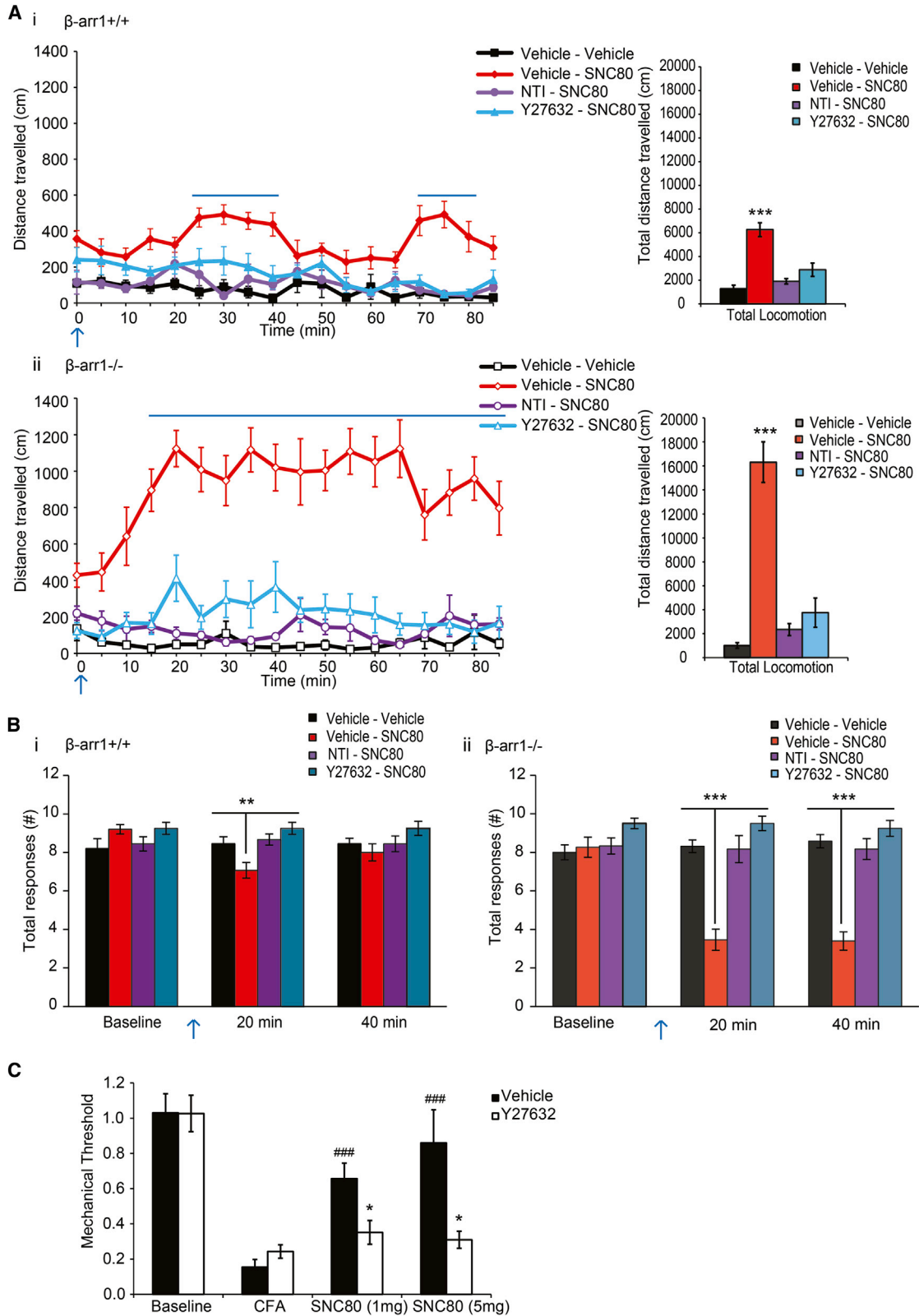
(legend on next page)

β-arr1^{+/+} mice 20 min after the injection. This was reversed by both the ROCK inhibitor (Y27632; 1 mg/kg administered intraperitoneally [i.p.]) and the delta antagonist, NTI (2 mg/kg s.c., $p < 0.001$ locomotion × treatment; Figure 5Ai). In contrast, β-arr1^{−/−} mice showed an enhanced locomotor effect of SNC80 seen both as a more rapid onset, occurring within 10 min of the SNC80 injection, and lasting considerably longer than in wild-type littermates ($p < 0.001$ versus β-arr1^{+/+}). Similar to +/+ mice, this was reversed by Y27632 and NTI ($p < 0.001$ locomotion × treatment; Figure 5Aii). To assess whether this inhibitory profile of Y27632 was due to nonspecific suppression of locomotor behavior, we tested the effect on Y27632 on the locomotor effects of fentanyl, a specific mu opioid receptor agonist. Fentanyl (0.4 mg/kg s.c.) induced an equal hyperlocomotor response in both genotypes that was not altered by Y27632 (1 mg/kg i.p.; Figure S5A). No gender-based differences in locomotion were observed in the SNC80-treated ($p = 0.69$ locomotion × gender) or fentanyl-treated ($p = 0.54$ locomotion × gender) groups.

In the second behavioral test of δOR function, the analgesic effect of SNC80 was assessed by mechanical pain, in which the number of paw withdrawals from ten applications of a 2 g von Frey filament was measured. We found that basal thresholds were not influenced by genotype and that wild-type mice showed a brief analgesic effect of SNC80 at the 20 min ($p < 0.05$ response × treatment), but not 40 min, time point (5 mg/kg s.c.; Figure 5Bi). In comparison, β-arr1^{−/−} mice showed enhanced analgesia or fewer responses 20 and 40 min after SNC80 ($p < 0.001$ response × treatment). This effect of SNC80 was reversed by Y27632 (1.5 mg/kg) and NTI (4 mg/kg; Figure 5Bii).

SNC80 produced some analgesia in naive wild-type mice (Figure 5Bi), but because chronic inflammatory pain results in enhanced δOR analgesia in wild-type mice (Pradhan et al., 2013), we next examined the role of ROCK in modulating δOR function in inflammatory pain. We injected saline or Y27632 (10 mg/kg i.p.) prior to injecting complete Freund's adjuvant (CFA; 10 μl) in the left hind paw of wild-type mice and at 12 hr intervals thereafter. After 48 hr, we assessed the effect of SNC80 (1 and 5 mg/kg s.c.) on the mechanical pain threshold in the Y27632- and saline-treated groups. We found that

Y27632 reduced the ability of SNC80 to relieve the mechanical hyperalgesia associated with chronic inflammatory pain ($p < 0.05$ versus vehicle; Figure 5C), highlighting the involvement of ROCK in the functional upregulation of δORs seen in this model.

We also assessed whether genetic background influenced the β-arr1 phenotype. Mice backcrossed to the C57Bl/6 background and lacking β-arr1 showed a similar enhanced response to SNC80 in both locomotor and acute pain studies (Figures S5B and S5C). Furthermore, this effect of SNC80 in β-arr1^{−/−} mice was specific to β-arr1; SNC80-induced locomotion was similar in β-arr2^{−/−}, β-arr2^{+/+}, and β-arr1^{+/+} mice (Figure S5B).

ORL1

We assessed the role of this pathway in modulating ORL1 function by measuring the locomotor effect of the ORL1 agonist, Ro 65-6570. This agonist is similar to Ro 64-6198, which has been shown to either induce hypolocomotion or have no locomotor effect in wild-type mice (Shoblock, 2007). Although wild-type mice showed no effect of Ro 65-6570 (1.5 mg/kg i.p.), β-arr1^{−/−} mice showed a hypolocomotor response ($p < 0.05$ locomotion × treatment), which was reversed by both Y27632 (0.5 mg/kg) and the ORL1 antagonist, J-113397 ($p < 0.05$ versus Ro 65-6570; Figure 6). Together, these data show enhanced ORL1 function in β-arr1^{−/−} mice that can be reversed by inhibiting ROCK.

DISCUSSION

In being able to scaffold with cofilin, the inactivating kinase, LIMK, and activating phosphatase, slingshot (SSL) or chronophin, arrestins can control the activity of cofilin to influence actin polymerization (Condeelis, 2001; Xiao et al., 2010; Zoudilova et al., 2007, 2010). This pathway enables a dynamic remodeling of the actin cytoskeleton in response to a chemotactic stimulus (Nishita et al., 2005) and, as we show here, modulates the function of some GPCRs; i.e., δOR and ORL1.

A Model of the Pathway

Based on GPCR inhibition of Ca^{2+} channels, a voltage-dependent and Gβγ-mediated response that modulates neurotransmitter release, we propose the following model (Figure 7). Under normal or wild-type conditions, agonist binding to an agonist such as the δOR activates cofilin through the

---

Figure 5. δOR Behaviors Are Regulated by β-arr1 and LIMK

(A) Two behavioral assays were used to assess δOR function. (i) Locomotion. β-arr1^{+/+} mice showed a hyperlocomotor response to subcutaneously administered SNC80 (3 mg/kg s.c., $p < 0.001$, $F_{5,28} = 13.125$, locomotion × treatment) that was reversed by both the ROCK inhibitor (Y27632 1 mg/kg i.p.) and the delta antagonist, naltrindole (2 mg/kg s.c.). β-arr1^{−/−} mice also showed a hyperlocomotor effect of SNC80 ($p < 0.001$, $F_{5,26} = 31.19$ locomotion × interaction), but this was enhanced ($p < 0.001$, $F_{1,9} = 25.79$ versus β-arr1^{+/+}), occurred more rapidly than the wild-type mice ($p < 0.001$, $F_{17,153} = 4.051$ versus β-arr1^{+/+}), and lasted for the duration of the test (90 min). This was similarly reversed by both Y27632 and naltrindole. The data show time (min) on the x axis and distance traveled (cm) on the y axis. The blue arrow represents the second of the two injections. The bar graphs depict the total locomotion over time.

(B) Mechanical analgesia was measured by the number of responses out of a total of ten applications of the same von Frey filament (2 g) to the plantar surface of the right hindpaw. β-arr1^{+/+} mice showed a small effect of SNC80 (5 mg/kg s.c., $p < 0.05$, $F_{3,39} = 3.388$, response × treatment) at the 20 min ($p < 0.01$, $F_{3,39} = 6.525$), but not the 40 min, time point. β-arr1^{−/−} mice, on the other hand, showed a greater response at both the 20 and 40 min time points after SNC80 administration ($p < 0.001$, $F_{2,37} = 43.37$, response × treatment). Y27632 (β-arr1^{+/+}: $p < 0.01$ versus SNC80, β-arr1^{−/−}: $p < 0.001$ versus SNC80) and naltrindole (β-arr1^{+/+}: $p < 0.01$ versus SNC80, β-arr1^{−/−}: $p < 0.001$ versus SNC80) reversed the antinociceptive effect of SNC80 in both β-arr1^{+/+} and β-arr1^{−/−} mice.

(C) We have previously shown that complete Freund's adjuvant (CFA) induced chronic pain decreases the mechanical threshold in the von Frey test of allodynia ($p < 0.001$, $F_{1,25} = 114.17$ versus baseline) in adult C57Bl6/J mice. This decrease is associated with a functional upregulation of δORs (Pradhan et al., 2013), as it can be reversed by SNC80 (1or 5 mg/kg s.c.; $p < 0.001$, $F_{1,23} = 33.84$ threshold × treatment) in wild-type mice. Administration of Y27632 (10 mg/kg i.p.) prior to injecting CFA, and at 12 hr intervals thereafter, did not alter the resultant hyperalgesia ($p = 0.563$, $F_{1,25} = 0.34$ versus vehicle) but did inhibit the effect of SNC80 (1 and 5 mg/kg; *$p < 0.05$ versus vehicle, ###$p < 0.001$ versus CFA). All data are shown as mean ± SEM.
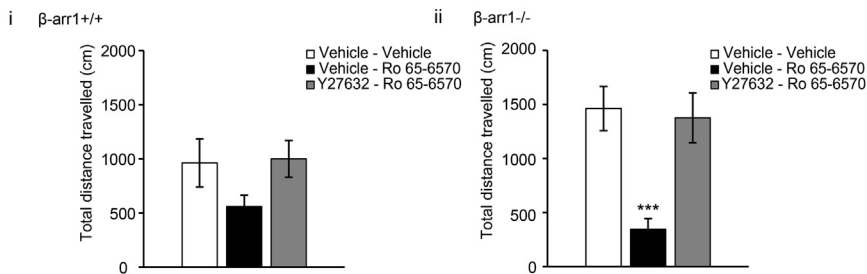
Figure 6. ORL1 Behavioral Responses Are Similarly Regulated by β-arr1 and LIMK

The bioavailable ORL1 agonist, Ro 65-6570 (1.5 mg/kg i.p.), did not alter the locomotor profile of β-arr1^{+/+} mice ($p = 0.54$, $F_{3,23} = 0.721$ locomotion × treatment) but induced a hypolocomotor response in β-arr1^{−/−} mice. This was reversed by Y27632 ($p < 0.05$, $F_{3,28} = 3.027$ locomotion × treatment). Data are shown as the total locomotor response following the injection of vehicle (vehicle), Ro 65-6570, or Y27632-Ro 65-6570 (Y27632-Ro 65) during the 45 min test period. All data are shown as mean ± SEM. ***$p < 0.001$ versus other treatment groups.

RhoA-ROCK-LIMK pathway. However, as β-arr1 is associated with LIMK and one of the cofilin phosphatases such as SSL (Xiao et al., 2010; Zoudilova et al., 2010), an enhanced but local activation of cofilin occurs. We propose that this results in controlled severing of F-actin and measured actin turnover to regulate the stability of a subset of actin filaments within the Golgi. This in turn controls the rate of export of δOR-containing cargo vesicles from the Golgi to the cell membrane to allow a limited response to a δOR agonist such as SNC80 (Figure 7A). In the absence of β-arr1, SNC80 similarly activates LIMK through the Rho-ROCK pathway, but without the regulatory control of β-arr1, cofilin is not dephosphorylated and activated by SNC80 (Lin et al., 2003). We propose that this leaves stable actin tracks in place, resulting in enhanced export of δORs from the Golgi to the plasma membrane to enhance δOR function (Figure 7B). This pathway can be blocked by inhibiting ROCK, the kinase responsible for phosphorylating LIMK and inactivating cofilin. In preventing agonist-induced activation of this pathway, we propose that agonist-induced turnover of a subset of actin filaments within the Golgi does not occur and additional receptors are not released to the cell membrane. Without this activation, the functional effect of the agonist is severely limited (Figure 7C).

δOR Trafficking and Function

δOR-VDCC inhibition is a rapid, voltage-dependent cascade that can be completely reversed by a high-voltage prepulse (data not shown). We have previously found that δOR-VDCC inhibition is positively correlated with δOR cell surface receptor levels (Walwyn et al., 2005). Furthermore, increased δOR-VDCC coupling is associated with enhanced δOR function (Pradhan et al., 2013) and, conversely, reduced δOR function is associated with reduced cell surface receptor levels (Scherrer et al., 2006). Together, this suggests a close relationship between cell surface receptor levels and δOR functionality, assessed either in vitro or in vivo. The data presented here suggest that the ROCK-LIMK-β-arr1 pathway is a critical mediator of this relationship and is required to obtain an initial functional response. Thereafter, the cooperative roles of β-arr1 in both desensitizing and modulating δOR trafficking may further regulate δOR signaling.

ORL1 Function

Similar to δORs, our data suggest that β-arr1 also regulates ORL1 function in a ROCK-, LIMK-, and actin-dependent manner.

However, this regulation is not evident in wild-type mice. It could be that ROCK, LIMK, and β-arr1 inhibit ORL1 function to non-detectable levels in wild-type neurons and mice. This is suggested from the low levels of ORL1-VDCC coupling in wild-type neurons (Figure 1) and the lack of a locomotor response to the ORL1 agonist used (Figure 6). Interestingly, ORL1 function has often been described in association with a pharmacological or behavioral stimulus (Bebawy et al., 2010; Shoblock, 2007), suggesting that this receptor, similar to δORs, may be upregulated under certain conditions.

Other Receptors or Channels that May Be Regulated by β-arr1, Cofilin, and LIMK

This fine-tuned control of actin polymerization to affect δOR and ORL1 function may similarly control ligand-dependent activation of other GPCRs such as dopamine receptor 1, neurotensin, or PAR$_2$, which are recruited from intracellular stores to the cell membrane "upon demand" (Brismar et al., 1998; Hein et al., 1994; Perron et al., 2006). Interestingly, many of these receptors share a common postendocytic fate of being degraded once internalized, suggesting that regulating the rate of receptor release may be important to allow sufficient GPCR activation. In providing a ligand-dependent spatiotemporal regulation of actin filaments, β-arr1 may also regulate the function of ligand-gated ion channels that may be rapidly trafficked to and from the synapse upon demand.

Other Regulators of the Pathway

We have examined GPCR activation of this pathway, but it is also possible that other receptors or molecules may be involved. For example, bradykinin or arachidonic acid has been shown to enhance δOR function (Patwardhan et al., 2005; Pettinger et al., 2013; Rowan et al., 2009). As kinins are involved in the hyperalgesic response to chronic pain (Ferreira et al., 2002), it is possible that bradykinin may activate this pathway in the CFA model of chronic pain.

Conclusions

Following agonist-receptor activation of downstream signaling cascades, GPCRs typically desensitize, becoming unable to induce the same signaling profile. In contrast, we have found that agonist binding with select GCPRs results in a functional upregulation of the receptor. This increases GPCR-Ca^{2+} channel inhibition and agonist-mediated behaviors, demonstrating how
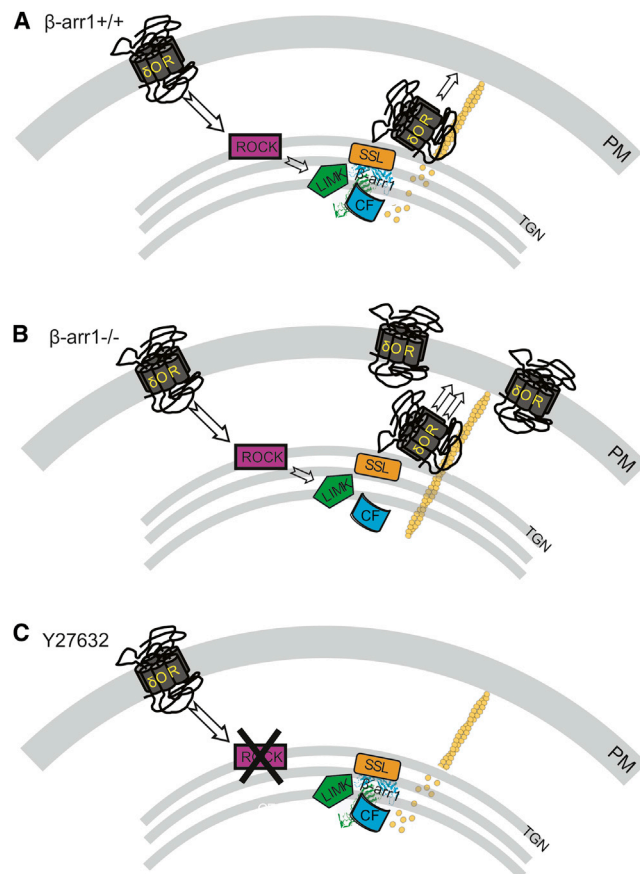
Figure 7. β-arr1 Regulation of GPCR Function

(A) β-arr1$^{+/+}$. In neurons containing β-arr1, the δOR agonist, SNC80, binds with δORs and activates ROCK. Because β-arr1 is associated with LIMK and one of the phosphatases (possibly SSL) within the trans-Golgi network (TGN), this activates cofilin to enhance actin filament severing and turnover to regulate δOR release to the cell membrane. PM, plasma membrane.

(B) β-arr1$^{-/-}$. Without the inhibitory control of β-arr1, LIMK phosphorylates and inactivates cofilin. This leaves stable actin tracks in place to allow unregulated but agonist-dependent δOR release to the plasma membrane in an agonist-dependent manner.

(C) Y27632. Preventing ROCK phosphorylation of LIMK by applying Y27632 prevents δOR activation of the pathway and agonist-induced release of δORs to the cell membrane.

this regulatory pathway allows these receptors to maintain or enhance receptor function.

EXPERIMENTAL PROCEDURES

Animals

All animal experiments were conducted in accordance with the *Guide for the Care and Use of Laboratory Animals* and followed institutionally approved animal care and use protocols. Mice lacking the β-arr1 (Conner et al., 1997) or δOR (Filliol et al., 2000) were fully backcrossed into the 129S6/SvEv or C57Bl/6 background. All animals used for the cellular experiments were bred from homozygous matings within one generation of heterozygous matings. For the behavioral experiments, 2- to 3-month-old equally distributed males and females were generated from heterozygous matings. Unless noted otherwise, all experiments used the 129S6/SvEv βarr1 line.

Compounds

Unless otherwise noted, all chemicals were obtained from Sigma, except for Y27632 (Selleckchem), SNC80, Naltrindole, ICI 174-864, Nociceptin, J113397, JTC801 (R&D Systems), S3 (Anaspec), and LIMK (Cytoskeleton).

Dorsal Root Ganglion Neuron Cultures

DRGs were harvested from early postnatal (p0–1) mice or adult (6- to 8-week-old) mice. The DRGs were enzymatically and physically dissociated and plated in different formats and densities for different experiments. For electrophysiology experiments, 5×10^4 dissociated cells were plated on poly-D-lysine-coated (Sigma) and laminin-coated (Becton Dickenson) coverslips (10 mm diameter) in the center of 35 mm MatTek dishes. Lentiviral transduction was performed at the time of plating by adding 50 ng p24/plate to each plate. For flow cytometry experiments, 1×10^6 cells were plated in a similarly coated 15 mm MatTek dish. The cells were cultured in 2 ml of Neurobasal A, B27, GlutaMAX (0.5 mM), and antibiotic-antimycotic (12 U/ml) media (Life Technologies) containing nerve growth factor (10 μg/ml, Roche) and kept at 37°C and 5% CO$_2$. Electrophysiological assessment of endogenous δOR function was performed within 24 hr of plating, and for those in which receptors were overexpressed, 72–96 hr thereafter. Flow cytometry was performed within 48 hr of plating.

Electrophysiology

The whole-cell patch-clamp technique was used to record voltage-dependent Ca^{2+} channel (VDCC) activity from DRG neurons (Axopatch 200A amplifier, Molecular Dynamics) as previously described (Walwyn et al., 2007). At the time of recording, the culture medium was replaced by an external solution that contained (in mM) 130 TEA-Cl, 10 CaCl$_2$, 5 HEPES, 25 D-glucose, and 2.5×10^{-4} tetrodotoxin (pH 7.2). Recording electrodes contained (in mM) 105 CsCl, 40 HEPES, 5 D-glucose, 2.5 MgCl$_2$, 10 EGTA, 2 Mg^{2+}-ATP, and 0.5 Na$^+$-GTP (pH 7.2). Ca^{2+} currents were activated by depolarizing neurons from −80 mV to 10 mV for 100 ms at 20 s intervals. Recordings that exhibited marked rundown were discarded. Stable recordings were fitted by a linear function to compare, by extrapolation, control current amplitude to the current amplitude recorded in the presence of the agonist. Data are expressed as mean ± SEM and were compared using ANOVA with a post hoc Scheffé test.

Cofilin Dephosphorylation

Wild-type MEFs or βarr1$^{-/-}$ MEFs were treated with SNC80 for 0–120 min, lysed, and analyzed by SDS-PAGE followed by western blotting with antibodies to phosphocofilin (rabbit polyclonal, 1:1,000; Cell Signaling) or total cofilin (mouse monoclonal, 1:500; BD Biosciences) and analyzed as previously described (Zoudilova et al., 2007). The data are expressed as the mean ± SEM, and differences between groups were determined by one-way ANOVA (Prism v5.03) with significance accepted at p < 0.05.

Flow Cytometry

After 48 hr in vitro, β-arr1$^{+/+}$ and β-arr1$^{-/-}$ or δOR$^{+/+}$ and δOR$^{-/-}$ DRG neurons were harvested and processed for δOR fluorescent labeling in nonfixed cells using a primary antibody to the N terminus of the δOR (MBL) and an allophycocyanin (APC)-conjugated secondary antibody (BD Biosciences) as previously described (Walwyn et al., 2009). The data are expressed as the mean ± SEM, and differences between groups were determined by one-way ANOVA or paired Student's t test with significance accepted at p < 0.05 (Analyze-it Software).

Behavioral Tests

Two- to 3-month-old β-arr1$^{-/-}$ and β-arr1$^{+/+}$ littermates of both genders were used for the following behavioral effects.

Locomotion

Because SNC80 is known to increase locomotor behavior, this effect was measured after 30 min of habituation to the test environment and the response to SNC80 15 min after the injection of the δOR antagonist naltrindole, the ROCK inhibitor Y27632, or vehicle, delivered s.c. or i.p., and measured over the following 90 min. This behavior was recorded in 27 × 27 cm plastic boxes by live tracking using an infrared camera and Ethovision XT (Noldus). Because ORL1 agonists can induce a hypolocomotor response, this effect was tested

by injecting a bioavailable ORL1 agonist, Ro 65-6570 (1.5 mg/kg i.p.) after 15 min of habituation and for the following 45 min. The ROCK inhibitor Y27632, the ORL1 antagonist J-113397, or vehicle was injected 15 min prior to Ro 65-6570.

Mechanical Pain

After 2 days of habituation to the test environment, the number of responses (defined as a lifting or shaking of the paw upon stimulation of the plantar surface), out of a total of ten repetitions to the 2 g von Frey filament was measured. Basal responses to the 2 g filament were acquired prior to the injections, and the effect was tested 20 and 40 min thereafter.

CFA

Wild-type mice were habituated for 3 days prior to obtaining the basal mechanical threshold by the up/down method (Chaplan et al., 1994). Saline or Y27632 (10 mg/kg i.p.) was injected prior to assessing the basal response, prior to the CFA injection (10 μl in the left hind paw), and at 12 hr intervals thereafter. After 48 hr, the mechanical pain threshold was assessed and the effect of SNC80 (1 and 5 mg/kg s.c.) determined. Data are expressed as mean ± SEM, and differences between groups were analyzed by ANOVA with repeated-measures and factorial analysis at each time point (Stat View v5).

SUPPLEMENTAL INFORMATION

Supplemental information includes Supplemental Experimental Procedures and five figures and can be found with this article online at http://dx.doi.org/10.1016/j.celrep.2013.10.015.

REFERENCES

Achour, L., Labbé-Jullié, C., Scott, M.G., and Marullo, S. (2008). An escort for GPCRs: implications for regulation of receptor density at the cell surface. Trends Pharmacol. Sci. 29, 528–535.

Ahmed, Z., Douglas, M.R., Read, M.L., Berry, M., and Logan, A. (2011). Citron kinase regulates axon growth through a pathway that converges on cofilin downstream of RhoA. Neurobiol. Dis. 41, 421–429.

Aizawa, H., Wakatsuki, S., Ishii, A., Moriyama, K., Sasaki, Y., Ohashi, K., Sekine-Aizawa, Y., Sehara-Fujisawa, A., Mizuno, K., Goshima, Y., and Yahara, I. (2001). Phosphorylation of cofilin by LIM-kinase is necessary for semaphorin 3A-induced growth cone collapse. Nat. Neurosci. 4, 367–373.

Bebawy, D., Marquez, P., Samboul, S., Parikh, D., Hamid, A., and Lutfy, K. (2010). Orphanin FQ/nociceptin not only blocks but also reverses behavioral adaptive changes induced by repeated cocaine in mice. Biol. Psychiatry 68, 223–230.

Brismar, H., Asghar, M., Carey, R.M., Greengard, P., and Aperia, A. (1998). Dopamine-induced recruitment of dopamine D1 receptors to the plasma membrane. Proc. Natl. Acad. Sci. USA 95, 5573–5578.

Bubb, M.R., Senderowicz, A.M., Sausville, E.A., Duncan, K.L., and Korn, E.D. (1994). Jasplakinolide, a cytotoxic natural product, induces actin polymerization and competitively inhibits the binding of phalloidin to F-actin. J. Biol. Chem. 269, 14869–14871.

Cahill, C.M., Holdridge, S.V., and Morinville, A. (2007). Trafficking of delta-opioid receptors and other G-protein-coupled receptors: implications for pain and analgesia. Trends Pharmacol. Sci. 28, 23–31.

Chaplan, S.R., Bach, F.W., Pogrel, J.W., Chung, J.M., and Yaksh, T.L. (1994). Quantitative assessment of tactile allodynia in the rat paw. J. Neurosci. Methods 53, 55–63.

Condeelis, J. (2001). How is actin polymerization nucleated in vivo? Trends Cell Biol. 11, 288–293.

Conner, D.A., Mathier, M.A., Mortensen, R.M., Christe, M., Vatner, S.F., Seidman, C.E., and Seidman, J.G. (1997). β-Arrestin1 knockout mice appear normal but demonstrate altered cardiac responses to β-adrenergic stimulation. Circ. Res. 81, 1021–1026.

DeFea, K.A. (2007). Stop that cell! Beta-arrestin-dependent chemotaxis: a tale of localized actin assembly and receptor desensitization. Annu. Rev. Physiol. 69, 535–560.

Dong, C., Filipeanu, C.M., Duvernay, M.T., and Wu, G. (2007). Regulation of G protein-coupled receptor export trafficking. Biochim. Biophys. Acta 1768, 853–870.

Egea, G., Lázaro-Diéguez, F., and Vilella, M. (2006). Actin dynamics at the Golgi complex in mammalian cells. Curr. Opin. Cell Biol. 18, 168–178.

Ferreira, J., Campos, M.M., Araújo, R., Bader, M., Pesquero, J.B., and Calixto, J.B. (2002). The use of kinin B1 and B2 receptor knockout mice and selective antagonists to characterize the nociceptive responses caused by kinins at the spinal level. Neuropharmacology 43, 1188–1197.

Filliol, D., Ghozland, S., Chluba, J., Martin, M., Matthes, H.W., Simonin, F., Befort, K., Gavériaux-Ruff, C., Dierich, A., LeMeur, M., et al. (2000). Mice deficient for delta- and mu-opioid receptors exhibit opposing alterations of emotional responses. Nat. Genet. 25, 195–200.

Heimann, K., Percival, J.M., Weinberger, R., Gunning, P., and Stow, J.L. (1999). Specific isoforms of actin-binding proteins on distinct populations of Golgi-derived vesicles. J. Biol. Chem. 274, 10743–10750.

Hein, L., Ishii, K., Coughlin, S.R., and Kobilka, B.K. (1994). Intracellular targeting and trafficking of thrombin receptors. A novel mechanism for resensitization of a G protein-coupled receptor. J. Biol. Chem. 269, 27719–27726.

Huff, T., Müller, C.S., Otto, A.M., Netzker, R., and Hannappel, E. (2001). beta-Thymosins, small acidic peptides with multiple functions. Int. J. Biochem. Cell Biol. 33, 205–220.

Komori, N., Matsumoto, H., Cain, S.D., Kahn, E.S., and Chung, K. (1999). Predominant presence of beta-arrestin-1 in small sensory neurons of rat dorsal root ganglia. Neuroscience 93, 1421–1426.

Lin, T., Zeng, L., Liu, Y., DeFea, K., Schwartz, M.A., Chien, S., and Shyy, J.Y. (2003). Rho-ROCK-LIMK-cofilin pathway regulates shear stress activation of sterol regulatory element binding proteins. Circ. Res. 92, 1296–1304.

Lowe, M. (2011). Structural organization of the Golgi apparatus. Curr. Opin. Cell Biol. 23, 85–93.

Morton, W.M., Ayscough, K.R., and McLaughlin, P.J. (2000). Latrunculin alters the actin-monomer subunit interface to prevent polymerization. Nat. Cell Biol. 2, 376–378, 10854330.

Nishita, M., Tomizawa, C., Yamamoto, M., Horita, Y., Ohashi, K., and Mizuno, K. (2005). Spatial and temporal regulation of cofilin activity by LIM kinase and Slingshot is critical for directional cell migration. J. Cell Biol. 171, 349–359.

Patwardhan, A.M., Berg, K.A., Akopain, A.N., Jeske, N.A., Gamper, N., Clarke, W.P., and Hargreaves, K.M. (2005). Bradykinin-induced functional competence and trafficking of the delta-opioid receptor in trigeminal nociceptors. J. Neurosci. 25, 8825–8832.

Perron, A., Sharif, N., Gendron, L., Lavallée, M., Stroh, T., Mazella, J., and Beaudet, A. (2006). Sustained neurotensin exposure promotes cell surface recruitment of NTS2 receptors. Biochem. Biophys. Res. Commun. 343, 799–808.

Pettinger, L., Gigout, S., Linley, J.E., and Gamper, N. (2013). Bradykinin controls pool size of sensory neurons expressing functional δ-opioid receptors. J. Neurosci. *33*, 10762–10771.

Pradhan, A., Smith, M., McGuire, B., Evans, C., and Walwyn, W. (2013). Chronic inflammatory injury results in increased coupling of delta opioid receptors to voltage-gated Ca2+ channels. Mol. Pain *9*, 8.

Qiu, Y., Loh, H.H., and Law, P.Y. (2007). Phosphorylation of the delta-opioid receptor regulates its beta-arrestins selectivity and subsequent receptor internalization and adenylyl cyclase desensitization. J. Biol. Chem. *282*, 22315–22323.

Rowan, M.P., Ruparel, N.B., Patwardhan, A.M., Berg, K.A., Clarke, W.P., and Hargreaves, K.M. (2009). Peripheral delta opioid receptors require priming for functional competence in vivo. Eur. J. Pharmacol. *602*, 283–287.

Salvarezza, S.B., Deborde, S., Schreiner, R., Campagne, F., Kessels, M.M., Qualmann, B., Caceres, A., Kreitzer, G., and Rodriguez-Boulan, E. (2009). LIM kinase 1 and cofilin regulate actin filament population required for dynamin-dependent apical carrier fission from the trans-Golgi network. Mol. Biol. Cell *20*, 438–451.

Scherrer, G., Tryoen-Tóth, P., Filliol, D., Matifas, A., Laustriat, D., Cao, Y.Q., Basbaum, A.I., Dierich, A., Vonesh, J.L., Gavériaux-Ruff, C., and Kieffer, B.L. (2006). Knockin mice expressing fluorescent delta-opioid receptors uncover G protein-coupled receptor dynamics in vivo. Proc. Natl. Acad. Sci. USA *103*, 9691–9696.

Shi, Y., Pontrello, C.G., DeFea, K.A., Reichardt, L.F., and Ethell, I.M. (2009). Focal adhesion kinase acts downstream of EphB receptors to maintain mature dendritic spines by regulating cofilin activity. J. Neurosci. *29*, 8129–8142.

Shoblock, J.R. (2007). The pharmacology of Ro 64-6198, a systemically active, nonpeptide NOP receptor (opiate receptor-like 1, ORL-1) agonist with diverse preclinical therapeutic activity. CNS Drug Rev. *13*, 107–136.

Tan, M., Walwyn, W.M., Evans, C.J., and Xie, C.W. (2009). p38 MAPK and beta-arrestin 2 mediate functional interactions between endogenous micro-opioid and alpha2A-adrenergic receptors in neurons. J. Biol. Chem. *284*, 6270–6281.

von Blume, J., Duran, J.M., Forlanelli, E., Alleaume, A.M., Egorov, M., Polishchuk, R., Molina, H., and Malhotra, V. (2009). Actin remodeling by ADF/cofilin is required for cargo sorting at the trans-Golgi network. J. Cell Biol. *187*, 1055–1069.

Walwyn, W.M., Keith, D.E., Jr., Wei, W., Tan, A.M., Xie, C.W., Evans, C.J., Kieffer, B.L., and Maidment, N.T. (2004). Functional coupling, desensitization and internalization of virally expressed mu opioid receptors in cultured dorsal root ganglion neurons from mu opioid receptor knockout mice. Neuroscience *123*, 111–121.

Walwyn, W., Maidment, N.T., Sanders, M., Evans, C.J., Kieffer, B.L., and Hales, T.G. (2005). Induction of delta opioid receptor function by up-regulation of membrane receptors in mouse primary afferent neurons. Mol. Pharmacol. *68*, 1688–1698.

Walwyn, W., Evans, C.J., and Hales, T.G. (2007). Beta-arrestin2 and c-Src regulate the constitutive activity and recycling of mu opioid receptors in dorsal root ganglion neurons. J. Neurosci. *27*, 5092–5104.

Walwyn, W., John, S., Maga, M., Evans, C.J., and Hales, T.G. (2009). Delta receptors are required for full inhibitory coupling of mu-receptors to voltage-dependent Ca(2+) channels in dorsal root ganglion neurons. Mol. Pharmacol. *76*, 134–143.

Xiao, K., Sun, J., Kim, J., Rajagopal, S., Zhai, B., Villén, J., Haas, W., Kovacs, J.J., Shukla, A.K., Hara, M.R., et al. (2010). Global phosphorylation analysis of beta-arrestin-mediated signaling downstream of a seven transmembrane receptor (7TMR). Proc. Natl. Acad. Sci. USA *107*, 15299–15304.

Zoudilova, M., Kumar, P., Ge, L., Wang, P., Bokoch, G.M., and DeFea, K.A. (2007). Beta-arrestin-dependent regulation of the cofilin pathway downstream of protease-activated receptor-2. J. Biol. Chem. *282*, 20634–20646.

Zoudilova, M., Min, J., Richards, H.L., Carter, D., Huang, T., and DeFea, K.A. (2010). beta-Arrestins scaffold cofilin with chronophin to direct localized actin filament severing and membrane protrusions downstream of protease-activated receptor-2. J. Biol. Chem. *285*, 14318–14329.